94537-99-2; **11a**, 94570-75-9; **11b**, 94570-67-9; **11c**, 74468-76-1; **11d**, 94570-68-0; **13a**, 94570-69-1; **13b**, 74468-77-2; **13c**, 94570-70-4; **15a**, 66-71-7; **15c**, 94537-96-9; **15d**, 94537-97-0; **15e**, 94537-98-1; **15** (R = CH_2Cl), 87518-61-4; **16c**, 94570-71-5; **17a**, 94570-72-6; **17b**, 94570-73-7; **17c**, 94570-74-8; $CH_2(CO_2Me)_2$, 108-59-8; $CH_2(CO_2Et)_2$, 105-53-3; $CH_2(COPr\text{-}i)_2$, 13195-64-7; $PdCl_2$, 7647-10-1; Li_2PdCl_4, 15525-45-8; $PdCl_2(PhCN)_2$, 14220-64-5; Na_2PdCl_4, 13820-53-6; EtONa, 141-52-6.

Supplementary Material Available: Tables of IR frequencies of pyridine-, pyrazine-, 2,2'-bipyridine-, and 1,10-phenanthroline-based ligands and their complexes, coordinates of H atoms for complexes **11a**, **11d**, **13b**, and **17c**, bond distances and angles for **11a**, **11c**, **11d**, **13b**, and **17c**, anisotropic thermal parameters for complexes **11a**, **11c**, **11d**, and **17c**, and structure factors for **11a**, **11c**, **11d**, **13b**, and **17c** (98 pages). Ordering information is given on any current masthead page.

Contribution from the Department of Chemistry,
University of Virginia, Charlottesville, Virginia 22901

Carbon-Rich Metallacarboranes. 13.[1] Synthesis and Structure of Bis(carboranyl)cobalt Complexes Derived from $(C_2H_5)_4C_4B_8H_8^{2-}$

ZHU-TING WANG,[2] EKK SINN, and RUSSELL N. GRIMES*

Received June 26, 1984

The reaction of $CoCl_2$ with $Et_4C_4B_8H_8^{2-}$ ion in tetrahydrofuran produced two crystalline dicobalt complexes that were isolated by column and plate chromatography: red $(Et_4C_4B_8H_8)_2Co_2$ (**1**), 35% yield, and red-orange paramagnetic $(Et_4C_4B_8H_7)_2Co_2$ (**2a**), 15%. From two-dimensional (2D) ^{11}B-^{11}B NMR data, **1** is proposed to consist of a pair of 14-vertex *closo*-$Co_2C_4B_8$ polyhedra sharing a common Co-Co edge, a previously unknown geometry in metallacarborane chemistry. Electron pairing between the formal Co(II) centers is proposed to account for the observed diamagnetism. The same reaction, when followed by addition of $B_5H_8^-$ ion, generates several isolable complexes, including **1** (18%) and the minor products **2b** (an isomer of **2a**), $(Et_4C_4B_8H_8)$-$Co(Et_4C_4B_8H_7OC_4H_8)$ (**3a**), $(Et_4C_4B_8H_7)_2CoH$ (**4a**), and $(Et_4C_4B_4H_6)CoH(Et_4C_4B_8H_8)$ (**5**). Compound **2b** slowly rearranges at room temperature to an isomer, **2c**. Treatment of **1** with I_2 in acetone at 25 °C produces $(Et_4C_4B_8H_7)_2(OCMe_2)_2CoH$ (**3c**, 22%), isomers of $(Et_4C_4B_8H_7)_2(OH)Co$ (**3d**, 8%; **3e**, 9%), $(Et_4C_4B_8H_6OH)_2HCo$ (**3f**, 11%), and **2b** (19%). Products **2a**, **2b**, **2c**, and **4a** are proposed to have a direct B-B linkage between their carborane ligands. An X-ray crystallographic study of **3c** revealed that the carborane ligands are bridged by an acetone molecule via a B-O-B array in which the direct interligand boron-boron distance is 2.26 Å, considered weakly bonding. The second acetone is coordinated to a single boron atom on one of the cages, and the metal-bonded faces of the carborane ligands are inclined with a dihedral angle of 27.1°. The established and proposed structures are discussed in light of current cluster bonding theory, and implications concerning metal-promoted ligand fusion and coupling processes are considered. Crystal data: $[(C_2H_5)_4C_4B_8H_7]_2[OC(CH_3)_2]_2CoH$, M_r = 692, space group $P2_1/c$, a = 9.897 (7) Å, b = 12.316 (3) Å, c = 33.31 (2) Å, β = 92.35 (3)°, V = 4057 Å^3, Z = 4, R = 0.073 for 3054 reflections having $F_o^2 > 3\sigma(F_o^2)$.

Introduction

This series of papers is concerned with the structural and chemical consequences of high carbon content in polyhedral boron clusters. Formal replacement of boron by carbon in a borane framework increases the number of skeletal bonding electrons and hence, according to the polyhedral skeletal electron pair theory[3] (PSEPT), should lead to progressively more open cage geometry as the carbon/boron ratio increases, provided the framework composition is otherwise unchanged. Thus, $C_2B_{10}H_{12}$ with 26 skeletal electrons is a closed icosahedral cage; $C_4B_8H_{12}$ and its *C*-alkyl derivatives, with 28 electrons, are formally of the nido class and adopt open-cage geometries (but are fluxional in solution[4]). The $R_4C_4B_8H_8^{2-}$ dianions are 30-electron arachno systems whose geometries are still more open than the nido species, as deduced from X-ray structure determinations on a cobaltocenium derivative of $(CH_3)_4C_4B_8H_9^-$ and on several transition-metal π complexes of $R_4C_4B_8H_8^{2-}$ ligands.[4a,5]

While this general trend is in line with expectation from theory, the observed structures are often surprising and lend new insights into cluster bonding that are obtainable, at present, only through experiment—that is, via synthesis and structural characterization of specific compounds. Earlier reports from this laboratory[4a] have described the preparation and structures of a number of 11-14-vertex four-carbon metallocarboranes containing ML_n units, where M is Fe, Co, or Ni and L is an exo-polyhedral ligand such as C_5H_5. The present study was directed to bis(carboranyl)metal "commo"-type complexes, which contain two distinct metallacarborane cage systems joined at a common vertex. Species of this class whose carborane moiety is $R_2C_2B_4H_4^{2-}$ (R = alkyl), e.g., $H_2Fe(R_2C_2B_4H_4)_2$, undergo oxidative ligand fusion to form $R_4C_4B_8H_8$ carboranes;[4a,b] hence, it was of interest to determine if fusion could be similarly effected when one or both ligands is $R_4C_4B_8H_8^{2-}$.

In this paper we describe the synthesis and structural investigation of homo bis(carboranyl) complexes in which both ligands are C_4B_8 units; hetero-type species incorporating two different carborane systems are reported in the accompanying article.[6]

Results and Discussion

Reaction of $Et_4C_4B_8H_8^{2-}$ Ion with $CoCl_2$. The room-temperature interaction of a THF solution of $Na^+{}_2Et_4C_4B_8H_8^{2-}$ with a two- to threefold excess of $CoCl_2$ generates several crystalline colored compounds, of which two have been isolated in pure form by column and plate chromatography (Scheme I). The major product, red diamagnetic **1**, was characterized from its ^{11}B and ^1H FT NMR spectra (Table I), IR (Table II), ^1H FT NMR spectra, and mass spectra as $(Et_4C_4B_8H_8)_2Co_2$ (Figure 1, class 1). A second species, orange paramagnetic **2a**, exhibits no definable NMR spectra and has been characterized from its IR and mass spectra only. The chemical ionization (CI) mass spectrum

(1) Part 12: Maynard, R. B.; Wang, Z.-T.; Sinn, E.; Grimes, R. N. *Inorg. Chem.* **1983**, *22*, 873.
(2) Visiting scholar from the Institute of Chemistry, Academica Sinica, Beijing, China, 1981-1983.
(3) (a) Wade, K. *Adv. Inorg. Chem. Radiochem.* **1976**, *18*, 1. (b) Rudolph, R. W. *Acc. Chem. Res.* **1976**, *9*, 446. (c) Mingos, D. M. P. *Nature (London), Phys. Sci.* **1972**, *236*, 99. (d) O'Neill, M. E.; Wade, K. In "Metal Interactions with Boron Clusters"; Grimes, R. N., Ed.; Plenum Press: New York, 1982; Chapter 1, and references therein.
(4) (a) Grimes, R. N. *Adv. Inorg. Chem. Radiochem.* **1983**, *26*, 55 and references therein. (b) Maxwell, W. M.; Miller, V. R.; Grimes, R. N. *Inorg. Chem.* **1976**, *15*, 1343. (c) Venable, T. L.; Maynard, R. B.; Grimes, R. N. *J. Am. Chem. Soc.* **1984**, *106*, 6187.
(5) Grimes, R. N.; Pipal, J. R.; Sinn, E. *J. Am. Chem. Soc.* **1979**, *101*, 4172.
(6) Wang, Z.-T.; Sinn, E.; Grimes, R. N. *Inorg. Chem.*, following paper in this issue.

0020-1669/85/1324-0826$01.50/0

Table I. 115.8-MHz ^{11}B FT NMR Data

compd	solvent[a]	δ (J, Hz)[b,c]	rel area
$(Et_4C_4B_8H_8)_2Co_2$ (1)	A	23.7 (125), −3.9 (65), −7.8 (115), −23.9 (136)	1:2:3:2
$(Et_4C_4B_8H_7)_2Co_2$ (2b)	B	28.5 (s), 18.8 (123), 6.9 (s), [−3.8,[d] −8.1,[d] −7.7 (148)],[e] −21.0 (163), −25.1 (138), −27.6 (137), −30.2 (146)	1:1:1:[9]:1:1:1:1
$(Et_4C_4B_8H_7)_2Co_2$ (2c)	C	19.8 (124), 6.1 (s),[e] −1.0 (140), −4.5,[d] −13.2 (131), −15.4 (146), −18.1 (146), −23.3,[d] −24.5 (143), −28.9 (143)	1:3:1:2:2:1:1:1:2:2
$(Et_4C_4B_8H_7)_2(OCMe_2)_2CoH$ (3c)	C	27.1 (s), 16.2 (132), 6.6 (s), 3.8 (s), −4.1 (173), −6.5 (139), −7.6 (126), −8.7 (145), −12.2 (112), −13.0 (129), −14.3 (132), −20.3 (136), −26.0 (144), −28.1 (129), −29.1 (104)	1:1:1:1:2:1:1:1:1:1:1:1:1:1:1
$(Et_4C_4B_8H_7)_2(OH)Co$ (3d)	D	28.6 (s), 18.9 (s), [−4.1 (137), −6.8[d]],[e] [−11.2,[d] −15.4,[d] −16.8[d]],[e] −19.8,[d] −28.3 (141)	~1:1:5:8:2:3
$(Et_4C_4B_8H_7)_2(OH)Co$ (3e)	D	12.9 (s), 5.5 (s), 1.7 (146), −3.0 (130), −14.7 (149), −16.5 (186), −17.9 (150)	~1:1:1:1:2:2:2
$(Et_4C_4B_8H_6OH)_2HCo$ (3f)	D	12.0,[d] −3.7,[d] ~−12,[d] −17.3,[d] −19.5[d]	2:2:1:2:1
$(Et_4C_4B_8H_7)_2CoH$ (4a)	B	35.6 (s), 9.3 (160), 1.8 (167), −7.0 (146), −8.3 (163), −15.7 (159), −26.1 (162), −43.7 (148)	equal areas
$(Et_4C_4B_8H_8)CoH(Et_4C_4B_4H_6)$ (5)	C	32.7 (s), 19.0 (148), −10.3,[d] −23.7 (145), −25.9 (133)	1:1:6:2:2

[a] Legend: A = acetone; B = C_6D_6; C = CH_2Cl_2; D = $CDCl_3$. [b] Legend: s = singlet (no B-H coupling). [c] Chemical shifts relative to $BF_3{\cdot}O(C_2H_5)_2$. [d] J value not measurable. [e] Superimposed or overlapped peaks.

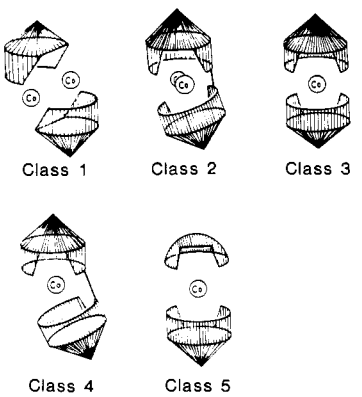

Figure 1. Schematic drawings of geometric modes (established or proposed) exhibited by $(C_4B_8)_2Co_2$, $(C_4B_8)_2Co$, and $(C_4B_8)Co(C_4B_4)$ complexes. Connections between cobalt and ligands are omitted for clarity, an artistic device having no bonding significance. Ligands represented are $Et_4C_4B_8H_8^{2-}$ or $(Et_4C_4B_8H_7)_2^{4-}$, except for the small ligand in class 5, which is $Et_4C_4B_4H_6^{2-}$. Complexes in this paper are labeled according to type; e.g., species **3a–f** are of class 3.

of **1** in CH_4 contains a high-mass cutoff at m/e 639, corresponding to the $^{59}Co_2{}^{13}C^{12}C_{23}{}^{11}B_{16}{}^{1}H_{56}{}^{+}$ parent ion, and the intensities in the parent envelope are in excellent agreement with the spectrum calculated from natural isotopic abundances for $[(C_2H_5)_4C_4B_8H_8]_2Co_2$; extensive fragmentation to form $(C_2H_5)_4C_4B_8H_8$ is indicated by a very intense peak group at m/e 261. The CI spectrum of **2a** similarly exhibits a very strong $(C_2H_5)_4C_4B_8H_8$ fragment, but the parent group cutoff is observed at m/e 637, indicating that **2a** has two fewer hydrogens than **1**. From this evidence, **2a** is proposed to have the composition $(Et_4C_4B_8H_7)_2Co_2$ with linked carborane ligands as suggested in Figure 1, class 2. The linked-cage feature turns out to be a ubiquitous one in this chemistry, as will be seen in the subsequent discussion.

Scheme I

$$Et_4C_4B_8H_8^{2-} + CoCl_2 \rightarrow (Et_4C_4B_8H_8)_2Co_2 \text{ (1) (red, 35\%)}$$
$$(Et_4C_4B_8H_7)_2Co_2 \text{ (2a) (orange-red, paramagnetic, 15\%)}$$

The formulas of **1** and **2a** suggest unusual, if not novel, metallacarborane structures. In the absence of an exo polyhedral ligand such as $C_5H_5^-$, it appears that both metals must be sandwiched between the two C_4B_8 carborane units, in a manner reminiscent of certain metallocenes such as $(C_5H_5)_2Pd_2(PR_3)_2$[7] and $(C_8H_8)_2Mo_2(CO)_4$,[8] in which two metal atoms are located between

Table II. Infrared Absorptions (cm^{-1})[a,b]

1	2990 vs, 2950 s, 2890 s, 2580 vs, 1720 m, 1555 m, 1460 s, 1380 s, 1335 w, 1220 w, br, 1125 w, 1070 w, 1020 w, 960 w, 940 w
2a	2940 vs, 2890 vs, 2830 vs, 2520 vs, 1440 s, 1360 s, 1330 m, 1260 w, 1100 m, 1040 m, 1000 s, 930 s, 915 s, 860 s, 700 m, 665 m, 630 m, 610 m
2b	3000 m, 2955 m, 2900 w, 2550 m, 1730 vs, 1460 m, br, 1370 s, 1227 s, 950 m, 920 m, 850 w, 530 m
2c	2960 s, 2900 s, 2850 w, 2830 w, 2540 m, 1720 m, 1630 w, br, 1445 m, 1365 m, 1275 m, br, 1175 w, 1100 m, 1075 m, 1050 vw, 1020 w, 940 m, 895 s
3a	2950 vs, 2910 s, 2850 m, 2540 vs, 1705 s, 1445 s, 1370 m, 1348 m, 1192 m, 1100 w, 1050 w, 1005 w, 935 m, 920 m, 860 w, 840 w
3c	3020 vs, 2980 vs, 2930 s, 2590 vs, 2410 w, 1750 s, 1630 w, br, 1480 s, 1403 s, 1350 w, 1305 s, 1270 w, 1255 s, 1225 s, 1145 s, 1090 m, 1055 m, 1010 m, 970 s, 940 m, 705 m
3d	3685 m, 3450 m, vb, 3020 s, 2980 s, 2920 m, 2600 s, 2420 w, 1740 s, 1680 w, br, 1475 s, 1400 m, 1390 m, 1245 w, 1210 w, 1140 m, 1115 m, 1060 w, 970 m, br, 930 w
3e	3710 m, 3450 m, vb, 3040 s, 3000 s, 2970 w, 2650 s, 1755 s, 1680 m, b, 1490 s, 1400 m, br, 1320 m, br, 1250 w, 1220 w, 1150 m, 1125 m, 1060 m, br, 990 m, 900 w
3f	3790 m, 3500 m, vb, 3040 s, 3000 s, 2940 m, 2640 s, 1750 m, br, 1670 m, br, 1490 m, 1410 m, 1330 m, br, 1260 w, 1150 m, 1120 m, 1070 m, br, 990 m
4a	3030 vs, 2995 vs, 2940 s, 2600 s, 2430 w, 1755 s, 1600 s, 1580 s, 1560 m, 1545 m, 1530 w, 1505 s, 1495 s, 1410 m, 1400 w, br, 1300 m, 1250 s, 1150 w, br, 1100 m, 1070 w, 1040 w, 1020 s, 970 m, 950 m
5	3030 vs, 2998 vs, 2940 s, 2625 vs, 2420 m, 1750 w, br, 1680 m, br, 1490 s, 1410 s, 1360 w, 1310 w, 1260 w, 1150 w, 1090 w, 1050 m, 980 m, 960 w, 910 w

[a] Key: vs = very strong; s = strong; m = medium; w = weak; br = broad. [b] CCl_4 solution vs. CCl_4.

hydrocarbon rings. The high-resolution ^{11}B and ^{1}H FT NMR data on **1** indicate the presence of a molecular mirror plane. Unfortunately, we have been unsuccessful in obtaining crystals suitable for X-ray diffraction studies; however, the homonuclear ^{11}B–^{11}B two-dimensional (2D) NMR spectrum (Figure 2) leads us to propose the "class 1" structure depicted schematically in Figure 1, with the detailed geometry shown in Figure 3. This structure can be described as a dimer composed of identical 12-vertex *arachno*-$Et_4C_4B_8H_8^{2-}$ ligands (derived from a 14-vertex closo polyhedron by removal of two vertices), each of which is face coordinated to both Co^{2+} ions. Equivalently, one can view the molecule as a pair of 14-vertex *closo*-$Co_2C_4B_8$ cages joined at a common Co–Co edge. Since the C_4B_8 ligands in **1** are identical and each is bisected by a mirror plane, this structure is consistent with the one-dimensional (1D) 115.8-MHz ^{11}B NMR

(7) Werner, H.; Kraus, H. J.; Schubert, U.; Ackermann, K. *Chem. Ber.* **1982**, *115*, 2905.
(8) Connop, A. H.; Kennedy, F. G.; Knox, S. A. R.; Riding, G. H. *J. Chem. Soc., Chem. Commun.* **1980**, 520.

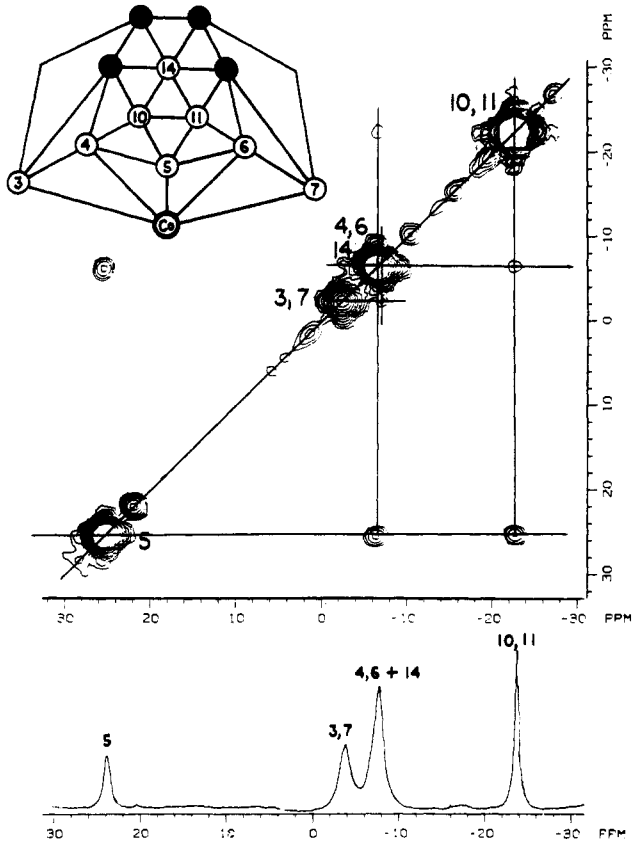

Figure 2. Two-dimensional ^{11}B–^{11}B FT NMR spectrum (115.8 MHz) of **1**. Peaks along the diagonal correspond to the normal proton-decoupled one-dimensional ^{11}B spectrum shown at bottom; off-diagonal "cross" peaks occur between scalar-coupled, hence adjacent, nuclei. The connectivity diagram at top left (carbon atoms shown as solid circles) is consistent with the spectrum and corresponds to the proposed structure in Figure 3.

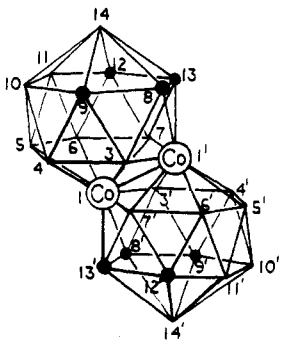

Figure 3. Proposed cage geometry of **1** with C–Et groups depicted as solid circles, other vertices being BH.

spectrum (Figure 2, bottom) provided that the area-3 peak at δ −7.8 is taken as superimposed area-2 and area-1 peaks.

The two-dimensional (2D) ^{11}B–^{11}B NMR spectrum[9] (Figure 2) supports the proposed structure for **1**, in that all expected "cross" (off-diagonal) peaks are observed except for that between the overlapped resonances at δ −7.8, which, of course, would be obscured. Although other cage geometries cannot be excluded, the requirement of mirror symmetry limits the placement of carbon atoms, and the high probability that at least two cage carbons will be on the open face of the $Et_4C_4B_8H_8^{2-}$ ligand[4a] points to the structure shown. Further, if the formal Co(II) centers are in close proximity as suggested, pairing of their odd electrons would remove the paramagnetism in conformity with observation. In compound **2a**, the observed paramagnetism indicates that electron pairing between the Co(II) atoms in that species does not take place; this in turn implies that the metal centers are separated, in contrast to **1** (a diamagnetic isomer of **2a** is discussed below). Several dimeric metallacarboranes obtained by Hawthorne et al., e.g., $[(C_6H_5)_3PRhC_2B_9H_{11}]_2$,[10] are structurally related to **1**, but the metal atoms in these species contain exo-polyhedral phosphine groups and are each face bonded to only one carborane ligand.

Reaction of $Et_4C_4B_8H_8^{2-}$, $CoCl_2$, and $B_5H_8^-$. Recent work in our laboratory has produced mixed-ligand "boranometallacarborane" complexes containing borane and carborane ligands bound to a common metal ion,[11] via treatment of $CoCl_2$ with $B_5H_8^-$ and $R_2C_2B_4H_4^{2-}$ ions in THF. In the present study, attempts to prepare analogous species containing C_4B_8 ligands gave only bis(carboranyl) complexes; however, since several of these products were not obtained in the absence of $B_5H_8^-$ (see previous reaction), it is evident that the borane anion does play a role in their formation (Scheme II). In these experiments the addition of $B_5H_8^-$ followed the reaction of $CoCl_2$ with the carborane ion, since the latter is the less reactive species.

Scheme II

$$Et_4C_4B_8H_8^{2-} + CoCl_2 \xrightarrow[THF]{B_5H_8^-}$$

$(Et_4C_4B_8H_8)_2Co_2$ (**1**) (red, 18%)
$(Et_4C_4B_8H_7)_2Co_2$ (**2b**) (golden, 2%)
$(Et_4C_4B_8H_8)Co(Et_4C_4B_8H_7OC_4H_8)$ (**3a**) (cranberry, 1%)
$(Et_4C_4B_8H_7)_2CoH$ (**4a**) (red-orange, 1%)
$(Et_4C_4B_4H_6)CoH(Et_4C_4B_8H_8)$ (**5**) (orange, 8%)

The main product is identical with the dicobalt complex **1** obtained from $Et_4C_4B_8H_8^{2-}$ and $CoCl_2$ alone. Of the remaining complexes, all isolated in low yield, **2b** is proposed to be an isomer of **2a** but the others are monocobalt species. Extensive discussion of these minor products is not warranted, particularly since the complexity of their ^{11}B NMR spectra prevents the assignment of unique geometries for most of them. However, if they are taken as a group, certain patterns of their composition and structure are apparent and deserve comment.

Compound **2b** exhibits a high-mass cutoff at m/e 637 (^{13}C peak) and a parent envelope corresponding to the formula $(Et_4C_4B_8H_7)_2Co_2$, and the ^{11}B NMR spectrum contains two singlets, suggesting a direct B–B link between the carborane ligand (Figure 1, class 2). Hence, **2b** is proposed to be isomeric with **2a**, both species having two fewer hydrogens than **1** by virtue of the interligand bond; in contrast to **2a**, however, **2b** is a diamagnetic species, implying a different geometry that permits intermetallic electron pairing in the latter compound. In hexane/toluene solution at room temperature, **2b** converts to a new isomer, **2c**, whose mass spectrum is close to that of **2b** but whose ^{11}B NMR spectrum (Table I) is clearly different.

Complex **3a** exhibits no measurable ^{11}B NMR spectra and is evidently paramagnetic, but from mass spectral evidence it is formulated as a THF-substituted monocobalt species having a nonlinked structure (Figure 1, class 3). Compound **4a** is interesting for several reasons. From its mass spectrum and ^{11}B NMR data (which contains eight area-1 peaks, one of which is a singlet assignable to a boron lacking a terminal hydrogen), the molecule is assigned a linked structure (Figure 1, class 4). Although the carborane ligands are presumed to be mutually rotated and probably tilted as well to facilitate intercage linkage, the boron NMR evidence indicates that they are identical, each boron atom in one ligand having its counterpart in the other. From the 2D boron NMR spectrum (Figure 4) the scope of possibilities is further narrowed, and the proposed structure is depicted in Figure

(9) The application of homonuclear ^{11}B 2D NMR spectroscopy to structure elucidation is described by: Venable, T. L.; Hutton, W. C.; Grimes, R. N. *J. Am. Chem. Soc.* **1984**, *106*, 29.

(10) (a) Behnken, P. E.; Knobler, C. B.; Hawthorne, M. F. *Angew. Chem., Int. Ed. Engl.* **1983**, *22*, 722. (b) Walker, J. A.; O'Con, C. A.; Zheng, L.; Knobler, C. B.; Hawthorne, M. F. *J. Chem. Soc., Chem. Commun.* **1983**, 803. (c) Baker, R. T.; King, R. E., III; Knobler, C. B.; O'Con, C. A.; Hawthorne, M. F. *J. Am. Chem. Soc.* **1978**, *100*, 8266.

(11) (a) Borodinsky, L.; Grimes, R. N. *Inorg. Chem.* **1982**, *21*, 1921. (b) Borodinsky, L.; Sinn, E.; Grimes, R. N. *Inorg. Chem.* **1982**, *21*, 1928.

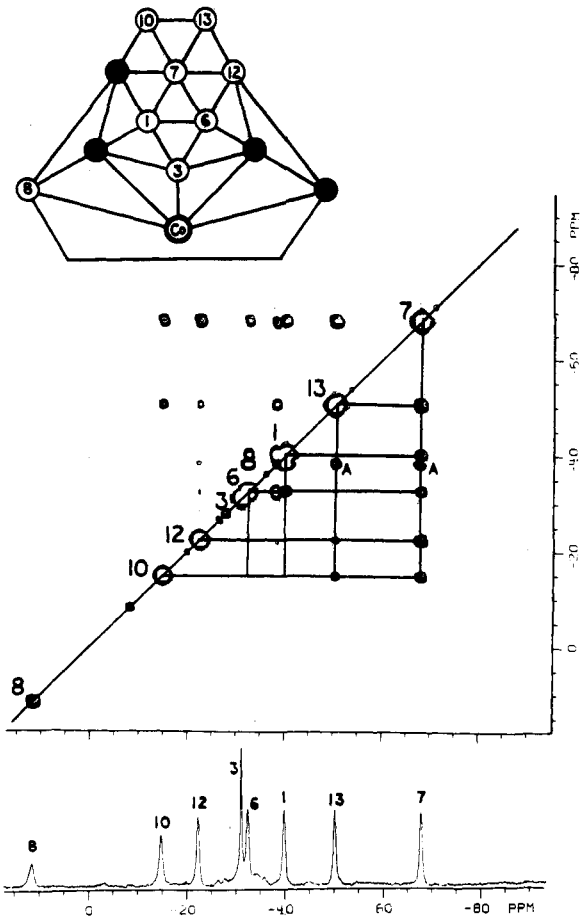

Figure 4. Two-dimensional ^{11}B–^{11}B FT NMR spectrum of **4a**, with proton-decoupled one-dimensional spectrum at bottom. The connectivity diagram, based on this spectrum, is consistent with the proposed structure in Figure 5.

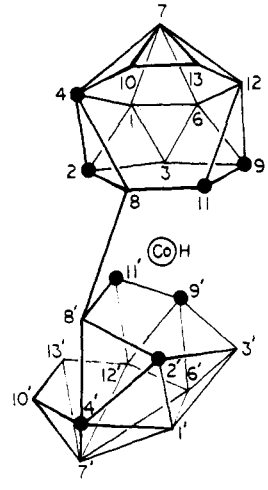

Figure 5. Proposed cage geometry of **4a**. The carborane ligands are identical, each boron nucleus having its equivalent counterpart in the other ligand. Each CoC_4B_8 unit is viewed as a 13-vertex arachno fragment of a 15-vertex closo polyhedron with vertices 14 and 15 vacant; cages are numbered accordingly (see discussion of complex **3c** in text). Cobalt–carborane bonding is omitted for clarity.

5. The shape of the postulated 12-vertex *arachno*-C_4B_8 ligands in **4a** is similar to that established via X-ray crystallography for a THF-substituted complex (**6a**), described elsewhere;[6] however, the cage carbon locations differ in the two molecules.

The ^{11}B NMR spectrum of **4a** is identical within experimental error with that of a product (**3b**) obtained in later work described in the following paper,[6] despite the fact that the compounds are clearly different. This unusual and initially perplexing situation was resolved by the 2D boron NMR spectra of the two species, which fortunately are dissimilar.

The orange complex **5** is tentatively identified as $(Et_4C_4B_4H_6)Co(Et_4C_4B_8H_8)$ from its mass spectrum, which contains a parent grouping (high m/e 535) whose intensities correspond to this composition, as well as an intense fragment assigned to $(Et_4C_4B_4H_6)Co$. The ^{11}B NMR spectrum is relatively simple, perhaps indicting overall mirror symmetry, but is otherwise uninformative. The formal $Et_4C_4B_4H_6^{2-}$ ligand, if it is indeed present, would be of the arachno class and hence is predicted from the PSEPT rules[3] to have the shape of a 10-vertex closo polyhedron minus two vertices.

Reaction of $(Et_4C_4B_8H_8)_2Co_2$ (1) with I_2. In order to investigate the possibility of effecting oxidative fusion or linkage of the carborane ligands in $(C_4B_8)_2$ metal complexes, the most accessible of these, **1**, was subjected to a variety of oxidants. In general, it was found that either no reaction ensued or the complex was degraded to noncharacterizable products (e.g., with $FeCl_3$ or O_2). Treatment with iodine in acetone solution, while it did not yield the desired fused, non-metal-containing carboranes, did produce several structurally interesting species containing acetone or hydroxyl substituents (Scheme III), one of which (**3c**) was characterized by X-ray diffraction.

Scheme III

$$(Et_4C_4B_8H_8)_2Co_2 \xrightarrow{I_2}$$
$$(Et_4C_4B_8H_7)_2Co_2 \text{ (2b) (golden, 19\%)}$$
$$(Et_4C_4B_8H_7)_2(COMe_2)_2CoH \text{ (3c) (purple, 22\%)}$$
$$(Et_4C_4B_8H_7)_2(OH)Co \text{ (3d) (green, 8\%)}$$
$$(Et_4C_4H_7)_2(OH)Co \text{ (3e) (cherry, 9\%)}$$
$$(Et_4C_4B_8H_6OH)_2HCo \text{ (3f) (purple, 11\%)}$$

When this reaction was repeated in methylene chloride solution, the same products were obtained with the exception of the acetone-containing species **3c**; hence, the source of hydroxyl in compounds **3d**, **3e**, and **3f** is not the solvent but is probably either atmospheric oxygen or adsorbed water on silica, which presumably reacts with one or more of the original products during chromatographic separation on silica. As this question was not central to our objectives in this project, it was not pursued.

Compound **2b** was identical with the species obtained in the earlier reaction (vide supra), as shown by its ^{11}B NMR and mass spectra and R_f value. The hydroxyl derivatives **3d**, **3e**, and **3f** exhibit mass spectra with intense parent groupings whose profiles correspond closely to those calculated from natural isotope abundances, with loss of hydrogen in the spectrometer evident in each case (see Experimental Section). The OH substituents give rise to singlets in the proton-coupled ^{11}B NMR spectra and also produce characteristic O–H stretching bands (>3000 cm^{-1}) in the IR spectra. In **3d** and **3e**, the molecular formulas suggest a bridging role for the single OH unit, linking the two ligands via a B–O–B interaction as has been described previously in certain dicarbollide cobalt complexes.[12] In **3f**, a simple formulation consistent with the data would have one terminal and one bridging OH group, but other arrangements are, of course, possible. In none of these three products can direct intercage B–B links be ruled out, but the nonlinked "class 3" structure is considered more likely in these cases.

The purplish red compound **3c** was characterized from its mass spectrum, which exhibits a cutoff at m/e 695 (^{13}C peak), and its pattern of abundances in the parent region, which corresponds almost exactly to those of the calculated spectrum. The ^{11}B NMR data exhibit three singlets in the proton-decoupled spectrum, which are assigned to three acetone-substituted boron atoms in the molecule. Given only two acetone groups, the spectrum implies that one $(CH_3)_2CO$ is bridging between the ligands and the other occupies a terminal (nonbridging) location. This placement was confirmed by an X-ray diffraction study of **3c**, which revealed

(12) Plesek, J.; Hermanek, S.; Base, K.; Todd, L. J.; Wright, W. F. *Collect. Czech. Chem. Commun.* **1976**, *41*, 3509 and references therein.

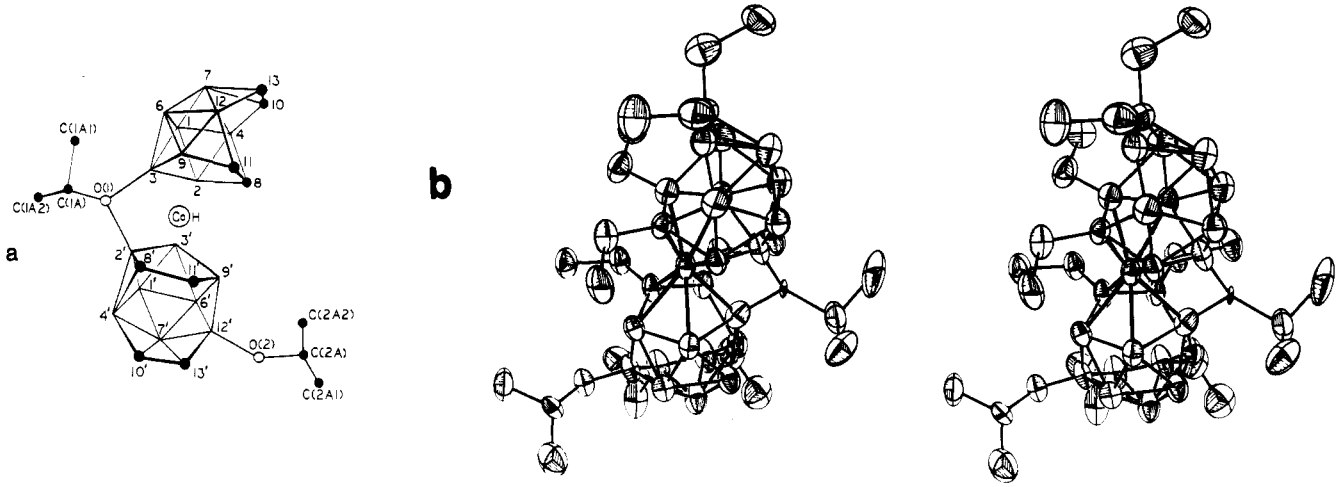

Figure 6. (a) Structure of **3c** showing cage numbering based on 13-vertex arachno geometry for CoC_4B_8 units. Cobalt–carborane bonding is omitted for clarity. (b) Stereoview of molecular structure of **3c**.

Table III. Experimental Parameters and Crystal Data

space group	$P2_1/c$	Z	4
a, Å	9.897 (7)	D(calcd), g cm^{-3}	1.13
b, Å	12.316 (3)	μ, cm^{-1}	4.7
c, Å	33.31 (2)	max trans coeff[a]	0.92
β, deg	92.35 (3)	min trans coeff	0.86
V, Å^3	4057	esd unit wt	2.3

[a] Crystal dimensions (mm from centroid): 100 (0.075), $\bar{1}00$ (0.075), 012 (0.25), $0\bar{1}\bar{2}$ (0.25), $01\bar{2}$ (0.45), $0\bar{1}2$ (0.45).

the structure depicted in Figure 6.

Crystallographic Study of $(Et_4C_4B_8H_7)_2(COMe_2)_2CoH$ (3c). Tables III–VI present the data collection parameters and crystal data, atomic coordinates, bond distances, and selected angles, while calculated planes are included in the supplementary data. The molecule consists of two open, irregular 12-vertex C_4B_8 ligands, each coordinated to the metal via a 5-membered face; the acetone substituents, as noted, occupy bridging and terminal locations. In the coding system introduced by one of us in a recent review,[4a] the two 13-vertex CoC_4B_8 cages are of types 5-*3334*(7) and 5-*3344*(6), respectively.[13] Despite the seeming complexity of this geometry, the basic shape can be accounted for, and usefully related to other metallacarborane structures, via simple PSEPT electron-counting arguments. Consider first the $Et_4C_4B_8H_8^{2-}$ ligand, a 30-electron system of the arachno class ($n + 3$ skeletal electron pairs). The complexation of two such ligands to a common Co^{3+} ion gives $(Et_4C_4B_8H_8)_2Co^-$, whose protonated derivative is $(Et_4C_4B_8H_8)_2CoH$. Such a complex would consist of two 13-vertex *nido*-CoC_4B_8 polyhedra (note that Co^{3+}, a d^6 ion, is formally a zero-electron donor to skeletal bonding and hence the electron population of each cage remains at 30 on addition of Co^{3+}, while the number of vertices increases from 12 to 13). A nido 13-vertex cage is predicted from PSEPT rules to have the shape of a 14-vertex closo polyhedron (bicapped hexagonal antiprism) minus one vertex, and this is in fact the established geometry of known 30-electron, 13-vertex metallacarboranes.[1,4a,6,14] In compound **3c**, however, the electron count is increased by a total of four, or two per cage[15] compared to $(Et_4C_4B_8H_8)_2CoH$, by virtue of the removal of two hydrogen atoms (loss of 2e) and the addition of two acetones, which contribute three electron pairs between them (gain of 6e). Thus, in **3c** the CoC_4B_8 cage units are formally 13-vertex, 32-electron arachno systems, which would be expected

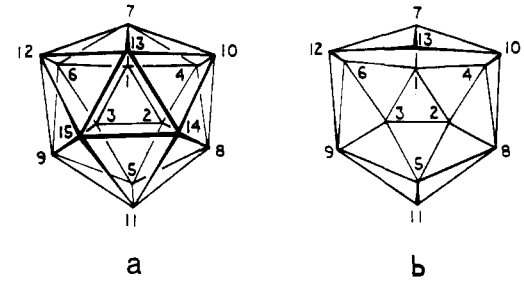

Figure 7. (a) Fifteen-vertex closo D_{3h} polyhedron with standard numbering, viewed down the three-fold axis. (b) Thirteen-vertex arachno fragment, obtained by removal of vertices 14 and 15. This cage numbering is maintained in each of the cage structures described herein. Connectivities may vary slightly, however; for example, in **3c**, connection 8–10 is nonbonding in both cages and connection 11–12 is bonding in one cage.

to adopt the shape of a closo 15-vertex polyhedron minus two vertices. Assuming the geometry of the highly symmetrical D_{3h} closo polyhedron proposed by Brown and Lipscomb[16] for the hypothetical $B_{15}H_{15}^{2-}$ ion, removal of vertices 14 and 15 as in Figure 7 yields a fragment corresponding reasonably closely to the open CoC_4B_8 cages observed in **3c**. The cage numbering (Figure 6) is based on this perception.

The two CoC_4B_8 cages are slightly different: that containing the terminal acetone (designated by "primed" atom labels) has a nonbonding distance (2.405 (8) Å) between C(11′) and B(12′), while the corresponding interaction in the other cage (C(11)–B(12)) is weakly bonding (1.960 (8) Å). As a consequence, the two cages have seven- and six-membered open faces, respectively. This effect probably arises from a transfer of electron density to B(12′) from its attached acetone substituent. In other respects, however, the atom connectivities in the two cages are the same; all eight skeletal carbon atoms are located on open faces, and each carborane ligand bonds to cobalt via a nearly planar CCBBB pentagonal face. The bridging acetone is linked to the two cages via nearly equivalent B–O bonds, but the $B_2O{=}C$ group is far from planar; C(1A) is 0.63 Å from the plane defined by B(3), B(2′), and O(1). Moreover, the sum of angles around O(1) is 351.3°, sufficiently less than 360° to suggest that the hybridization on oxygen is between sp^2 and sp^3. The constraining effect of the bridging acetone is shown by the tilt of the two carborane ligands. Thus, the dihedral angle formed by the B(2)–B(3)–B(9)–C(11)–C(8) face and its counterpart on the other ligand is 27.1°, an unusually large deviation from parallel orientation. This bending of the carborane ligands toward each other is manifested in a relatively short interligand B(3)–B(2′) distance (2.259 (9)

(13) In this scheme (ref 4a, p 68–69), the coordination number (CN) of the metal (with respect to cage connections only) is given to the left of the hyphen, while the CN's of the four cage carbons are to the right. Underlined digits indicate location on an open face, and the number in parentheses denotes the number of atoms on the open face.
(14) Grimes, R. N.; Sinn, E.; Pipal, J. R. *Inorg. Chem.* **1980**, *19*, 2087.
(15) The argument assumes, for the sake of simplicity, that the four-electron gain is divided evenly between the cages.
(16) Brown, L. D.; Lipscomb, W. N. *Inorg. Chem.* **1977**, *16*, 2989.

Table IV. Positional Parameters for $[(C_2H_5)_4C_4B_8H_7]_2[OC(CH_3)_2]_2CoH$ (3c)

atom	x	y	z	atom	x	y	z
Co	0.0041 (1)	0.1356 (1)	0.12501 (3)	B(2′)	−0.0349 (10)	0.2470 (10)	0.1686 (3)
O(2)	−0.2652 (5)	0.4079 (5)	0.0488 (2)	B(3′)	0.0473 (10)	0.3043 (10)	0.1240 (3)
O(1)	0.0399 (5)	0.1881 (5)	0.2012 (2)	B(4′)	−0.1855 (11)	0.3247 (10)	0.1772 (3)
C(1A)	0.0916 (11)	0.2503 (9)	0.2381 (3)	B(6′)	−0.0608 (10)	0.4052 (10)	0.1074 (3)
C(1A1)	0.0976 (12)	0.1600 (12)	0.2694 (3)	B(7′)	−0.1876 (11)	0.4463 (11)	0.1406 (3)
C(1A2)	0.2283 (11)	0.3038 (10)	0.2305 (4)	B(9′)	−0.0763 (10)	0.2714 (9)	0.0857 (3)
C(2A)	−0.1739 (10)	0.4518 (8)	0.0193 (3)	B(12′)	−0.2243 (10)	0.3759 (11)	0.0873 (3)
C(2A1)	−0.1992 (12)	0.5731 (12)	0.0194 (4)	H(1)	0.350 (7)	0.092 (6)	0.196 (2)
C(2A2)	−0.2141 (12)	0.4003 (11)	−0.0207 (3)	H(2)	0.297 (8)	0.188 (7)	0.132 (3)
C(8)	0.1501 (8)	0.0448 (7)	0.0993 (2)	H(4)	0.423 (6)	0.042 (5)	0.123 (2)
C(M8)	0.1843 (8)	0.0631 (8)	0.0554 (3)	H(7)	0.357 (7)	−0.124 (7)	0.196 (2)
C(E8)	0.2781 (9)	0.1562 (9)	0.0474 (3)	H(9)	−0.095 (7)	−0.052 (6)	0.166 (2)
C(10)	0.3298 (8)	−0.1192 (8)	0.1232 (2)	H(12)	0.018 (8)	−0.213 (7)	0.162 (3)
C(M10)	0.4651 (10)	−0.1667 (8)	0.1109 (3)	H(3′)	0.152 (6)	0.345 (6)	0.123 (2)
C(E10)	0.4837 (11)	−0.1616 (11)	0.0668 (3)	H(4′)	−0.183 (7)	0.312 (6)	0.211 (2)
C(11)	0.0405 (8)	−0.0261 (8)	0.1094 (3)	H(6′)	−0.003 (7)	0.470 (6)	0.090 (2)
C(M11)	−0.0458 (10)	−0.0824 (9)	0.0758 (3)	H(7′)	−0.229 (8)	0.522 (8)	0.152 (3)
C(13)	0.2199 (9)	−0.1837 (7)	0.1314 (3)	H(9′)	−0.058 (6)	0.259 (5)	0.052 (2)
C(M13)	0.2239 (10)	−0.3099 (9)	0.1302 (4)	H(8M1)	0.105 (7)	0.066 (6)	0.038 (2)
C(E13)	0.2634 (12)	−0.3648 (10)	0.1700 (3)	H(8M2)	0.229 (7)	−0.005 (7)	0.047 (2)
C(8′)	−0.1741 (7)	0.1867 (8)	0.1487 (2)	H(10M1)	0.468 (7)	−0.234 (6)	0.120 (2)
C(M8′)	−0.2787 (8)	0.1159 (9)	0.1694 (3)	H(10M2)	0.538 (7)	−0.127 (7)	0.126 (2)
C(E8′)	−0.2591 (10)	0.0896 (10)	0.2151 (3)	H(13M1)	0.292 (7)	−0.327 (6)	0.112 (2)
C(10′)	−0.3257 (9)	0.3611 (10)	0.1565 (3)	H(13M2)	0.136 (7)	−0.346 (7)	0.123 (2)
C(M10′)	−0.4533 (12)	0.3722 (12)	0.1880 (4)	H(M8′1)	−0.289 (8)	0.045 (7)	0.155 (3)
C(E10′)	−0.4209 (12)	0.4658 (12)	0.2085 (4)	H(M8′2)	−0.368 (7)	0.152 (6)	0.165 (2)
C(11′)	−0.1818 (8)	0.1897 (8)	0.1055 (2)	H(1A11)	0.117 (6)	0.193 (6)	0.291 (2)
C(M11′)	−0.2926 (8)	0.1298 (9)	0.0834 (3)	H(1A12)	0.166 (8)	0.096 (7)	0.265 (3)
C(E11′)	−0.2934 (10)	0.1331 (10)	0.0372 (3)	H(1A13)	0.010 (8)	0.125 (7)	0.277 (3)
C(13′)	−0.3441 (8)	0.3853 (10)	0.1163 (3)	H(2A11)	−0.144 (7)	0.597 (6)	−0.001 (2)
C(M13′)	−0.4686 (9)	0.4749 (12)	0.1010 (3)	H(2A12)	−0.176 (8)	0.611 (7)	0.044 (3)
C(E13′)	−0.5421 (15)	0.3861 (12)	0.0883 (4)	H(2A13)	−0.295 (9)	0.594 (8)	0.013 (3)
C(E11)	−0.142 (2)	−0.169 (2)	0.0906 (7)	H(E81)	0.328 (8)	0.145 (7)	0.020 (3)
C(E12)	0.007 (2)	−0.171 (2)	0.0550 (6)	H(E82)	0.369 (8)	0.172 (7)	0.068 (3)
B(1)	0.2636 (10)	0.0420 (9)	0.1809 (3)	H(E83)	0.236 (10)	0.226 (9)	0.052 (3)
B(2)	0.2161 (9)	0.1199 (9)	0.1371 (3)	H(E8′2)	−0.156 (7)	0.063 (7)	0.224 (2)
B(3)	0.0990 (10)	0.1002 (10)	0.1779 (3)	H(E8′3)	−0.270 (8)	0.149 (7)	0.230 (3)
B(4)	0.3257 (9)	0.0018 (9)	0.1306 (3)	H(M11′1)	−0.379 (8)	0.161 (7)	0.091 (2)
B(6)	0.1253 (11)	−0.0396 (10)	0.1932 (3)	H(M11′2)	−0.291 (8)	0.050 (7)	0.091 (2)
B(7)	0.2759 (11)	−0.1026 (11)	0.1748 (3)	H(E11′1)	−0.399 (8)	0.112 (7)	0.025 (3)
B(9)	−0.0049 (10)	−0.0139 (10)	0.1552 (3)	H(E11′2)	−0.217 (8)	0.078 (8)	0.027 (3)
B(12)	0.0912 (11)	−0.1362 (11)	0.1497 (4)	H(E11′3)	−0.274 (10)	0.202 (9)	0.028 (3)
B(1′)	−0.0339 (10)	0.3892 (10)	0.1599 (3)				

Å), which is, in fact, within weakly bonding range. This particular observation carries implications concerning ligand fusion to which we shall return.

The terminally bonded acetone substituent exhibits normal distances and angles, the comparatively short O(2)–B(12′) distance of 1.384 (6) Å and C(2A)–O(2)–B(12) angle of 124° suggesting sp^2 hybridization on oxygen. Bond distances within the two cages are within normal ranges (although there are several unusually long bonds, e.g., B–B interactions of 2 Å or more). It is noteworthy that the framework C–C bonds are all short (1.38–1.44 Å), indicative of local carbon–carbon multiple bonding, as is commonly observed for C–C edges on open faces in carboranes.[4a]

The formula of the molecule contains 14 hydrogen atoms other than those associated with acetone and ethyl groups, of which 13 occupy terminal BH locations; the remaining hydrogen, which probably resides in the vicinity of the metal,[17] was not located in the X-ray study.

Concluding Observations

The crystallographically determined structure of **3c** further extends our knowledge of the cage geometry of large carbon-rich metallacarborane systems and underlines previously noted trends,[4a] e.g., the propensity of carbon to adopt low-coordinate vertices on open faces. Moreover, it is apparent that the skeletal electron-counting rules are applicable even to systems as large as the 13-vertex, 32-electron arachno cages in **3c**. However, as has been noted elsewhere,[4a] in these complex species the rules serve mainly as a structural rationale and cannot (for now) predict specific cage geometries a priori.

Probably the most significant general finding in this work is the evidence for the formation of interligand B–B links in bis(carboranyl)metal complexes, inasmuch as this bears on the mechanism(s) of metal-promoted linkage and fusion of boranes and carboranes.[18] At least one structurally confirmed example of such direct linkage had been found prior to the present work, namely $(\eta^5\text{-}C_5Me_5)_2Co_3Me_4C_4B_8H_7$,[19] and in **3c**, as noted above, the acetone-bridged boron atoms on separate cages are within weak bonding distance. In the prototypical oxidative-fusion reaction, the conversion of $(R_2C_2B_4H_4)_2FeH_2$ to $R_4C_4B_8H_8$, detailed studies have established that the fusion process is intramolecular and hence is initiated while the ligands are still attached to the metal.[18] In the $(C_4B_8)_2Co$ complexes, the large steric bulk of the ligands would facilitate bringing them within coupling distance; oxidative removal of terminal hydrogens, with solvent playing a role (as suggested by the structure of **3c**), could lead to linked or even fused carborane products (although we consider the latter less likely with large cages). Several of these complexes appear to represent intermediate stages in this process, which are stable toward air oxidation and hence do not proceed further toward elimination of the metal and completion of the fusion process. Nevertheless, evidence for the formation of fused or coupled carborane products in mixed-ligand reactions has been obtained, as reported in the accompanying paper.

(17) Pipal, J. R.; Grimes, R. N. *Inorg. Chem.* **1979**, *18*, 263.

(18) Maynard, R. B.; Grimes, R. N. *J. Am. Chem. Soc.* **1982**, *104*, 5983.

(19) Finster, D. C.; Sinn, E.; Grimes, R. N. *J. Am. Chem. Soc.* **1981**, *103*, 1399.

Table V. Bond Lengths (Å) for 3c

Co-C(8)	2.043 (4)	B(2)-B(3)	1.840 (7)
Co-C(11)	2.093 (5)	B(2)-B(4)	1.833 (8)
Co-B(2)	2.129 (5)	B(3)-B(6)	1.812 (9)
Co-B(3)	2.011 (5)	B(3)-B(9)	1.882 (8)
Co-B(9)	2.101 (6)	B(4)-B(7)	2.032 (8)
Co-B(2′)	2.046 (6)	B(6)-B(7)	1.809 (8)
Co-B(3′)	2.121 (6)	B(6)-B(9)	1.797 (8)
Co-B(9′)	2.249 (6)	B(6)-B(12)	1.893 (8)
Co-C(8′)	2.060 (4)	B(7)-B(12)	2.022 (8)
Co-C(11′)	2.038 (4)	B(9)-B(12)	1.795 (9)
O(1)-C(1A)	1.522 (6)	B(1′)-B(2′)	1.775 (9)
O(1)-B(3)	1.466 (7)	B(1′)-B(3′)	1.802 (8)
O(1)-B(2′)	1.479 (7)	B(1′)-B(4′)	1.813 (8)
O(2)-C(2A)	1.467 (5)	B(1′)-B(6′)	1.768 (7)
O(2)-B(12′)	1.384 (6)	B(1′)-B(7′)	1.771 (8)
C(1A)-C(1A1)	1.523 (9)	B(2′)-B(3′)	1.861 (8)
C(1A)-C(1A2)	1.535 (7)	B(2′)-B(4′)	1.804 (8)
C(2A)-C(2A1)	1.515 (8)	B(2′)-C(8′)	1.677 (7)
C(2A)-C(2A2)	1.514 (7)	B(3′)-B(6′)	1.716 (8)
C(8)-C(M8)	1.531 (6)	B(3′)-B(9′)	1.778 (7)
C(8)-C(11)	1.443 (6)	B(4′)-B(7′)	1.929 (9)
C(8)-B(2)	1.673 (6)	B(4′)-C(8′)	1.952 (8)
C(8)-B(4)	2.058 (7)	B(4′)-C(10′)	1.588 (7)
C(M8)-C(E8)	1.505 (7)	B(6′)-B(7′)	1.780 (8)
C(10)-C(M10)	1.533 (6)	B(6′)-B(9′)	1.804 (8)
C(10)-C(13)	1.382 (6)	B(6′)-B(12′)	1.763 (8)
C(10)-B(4)	1.511 (7)	B(7′)-B(12′)	1.997 (8)
C(10)-B(7)	1.834 (7)	B(7′)-C(10′)	1.819 (9)
C(M10)-C(E10)	1.490 (7)	B(7′)-C(13′)	1.876 (8)
C(11)-C(M11)	1.546 (6)	B(9′)-B(12′)	1.953 (8)
C(11)-B(9)	1.614 (6)	B(9′)-C(11′)	1.611 (7)
C(11)-B(12)	1.960 (8)	B(12′)-C(13′)	1.565 (7)
C(M11)-C(E11)	1.526 (11)	C(8′)-C(M8′)	1.539 (6)
C(M11)-C(E12)	1.407 (10)	C(8′)-C(11′)	1.439 (6)
C(13)-C(M13)	1.556 (7)	C(M8′)-C(E8′)	1.562 (6)
C(13)-B(7)	1.827 (8)	C(10′)-C(M10′)	1.681 (8)
C(13)-B(12)	1.550 (7)	C(10′)-C(13′)	1.375 (6)
C(M13)-C(E13)	1.523 (8)	C(M10′)-C(E10′)	1.371 (9)
B(1)-B(2)	1.794 (7)	C(11′)-C(M11′)	1.492 (6)
B(1)-B(3)	1.778 (8)	C(M11′)-C(E11′)	1.540 (6)
B(1)-B(4)	1.877 (8)	C(13′)-C(M13′)	1.717 (9)
B(1)-B(6)	1.759 (8)	C(M13′)-C(E13′)	1.371 (9)
B(1)-B(7)	1.797 (9)	B(3)-B(2′)	2.259 (9)

Experimental Section

Materials. Tetra-*C*-ethyl-2,3,7,8-tetracarbadodecaborane(12) ($Et_4C_4B_8H_8$) was prepared from *nido*-$Et_2C_2B_4H_6$ and $FeCl_2$ via the intermediate complex $(Et_2C_2B_4H_4)_2FeH_2$ as described elsewhere.[4b,20] Anhydrous $CoCl_2$ was prepared by dehydration of $CoCl_2 \cdot 6H_2O$ (Baker reagent grade). Naphthalene (Baker) and sodium hydride (Alfa) were used as received. All solvents were reagent grade, and tetrahydrofuran (THF) was dried over sodium metal and then over lithium hydride immediately prior to use. Column chromatography was conducted on silica gel 60 (Merck), and thin-layer chromatography (TLC) was performed on precoated plates of silica gel F-254 (Brinckmann Instruments, Inc.).

Instrumentation. ^{11}B and ^1H FT NMR spectra at 115.8 and 360 MHz, respectively, were obtained on a Nicolet Magnetics Corp. NT-360/Oxford spectrometer. Two-dimensional (2D) ^{11}B–^{11}B NMR spectra were produced on selected samples via a procedure described elsewhere.[9] Infrared spectra were recorded on a Perkin-Elmer Model 1430 spectrometer. Mass spectra were obtained in chemical ionization or electron-impact mode on a Finnegan MAT Model 4610 GC/MS spectrometer in the Department of Chemistry, or by Harvey Laboratories, Inc., Charlottesville, VA.

Reaction of $Na^+_2Et_4C_4B_8H_8^{2-}$ with $CoCl_2$ in THF. A 100-mL three-neck flask was charged with 1040 mg (4.0 mmol) of $Et_4C_4B_8H_8$, and to it was added on the vacuum line,[11a] at liquid-nitrogen temperature, 8.0 mmol of sodium naphthalenide ($NaC_{10}H_8$) in ca. 35 mL of dry THF. As it was warmed to room temperature, the initially dark green solution acquired the light yellow color of the $Et_4C_4B_8H_8^{2-}$ ion[21] (which can also appear with a greenish or brownish tinge if excess $NaC_{10}H_8$ is present). The mixture was cooled to −63 °C, and excess $CoCl_2$ (ca. 3 mmol) was added in vacuo.[11a] The mixture was stirred 2–4 h at room temperature (in some experiments the temperature was held at −63 °C during this period, with no observable difference in the products). The solvent was removed on a rotary evaporator and the residue extracted with CH_2Cl_2 and filtered through a 3-cm layer of silica gel to remove insolubles, after which the CH_2Cl_2 was removed from the filtrate by evaporation and the solid products were placed on a silica gel chromatographic column and eluted with *n*-hexane followed by 1:1 hexane/CH_2Cl_2, pure CH_2Cl_2, and 1:1 CH_2Cl_2/acetone. The combined material from the first three of these elutions was collected, the solvent removed, and the solid placed in the vacuum line and heated to 60 °C in vacuo to remove naphthalene by sublimation. The remaining solid was placed on a preparative TLC plate and developed in hexane to give red-orange $(Et_4C_4B_8H_7)_2Co_2$ (**2a**), yield 190 mg. Mass spectrum (CI in CH_4): cutoff at *m/e* 637 (parent, $^{13}C^{12}C_{23}{}^{11}B_{16}{}^1H_{54}{}^{59}Co_2{}^+$, with an intensity pattern corresponding to that calculated for $C_{24}B_{16}Co_2$). A large number of other bands containing very small amounts of material were observed but were not isolated or characterized.

The second fraction (CH_2Cl_2/acetone) from the column elution was purified by TLC in 1:1 hexane/toluene (R_f 0.42) to give red $(Et_4C_4B_8H_8)_2Co_2$ (**1**), yield 450 mg. Mass spectrum (CI): cutoff at *m/e* 639 (parent, $^{13}C^{13}C_{23}{}^{11}B_{16}{}^1H_{56}{}^{59}Co_2{}^+$, $C_{24}B_{16}Co_2$ pattern). ^1H NMR (acetone-d_6): δ 1.25 (CH_3), 2.14 (CH_2).

Reaction of $Na^+_2Et_4C_4B_8H_8^{2-}$ with $CoCl_2$ Followed by $Na^+B_5H_8^-$ in THF. The treatment of $Na^+_2Et_4C_4B_8H_8^{2-}$ with $CoCl_2$ was conducted as described in the preceding section, with use of identical quantities of reagents. The dark brown reaction mixture was stirred at room temperature for 2 h in vacuo and then frozen in liquid nitrogen, and 4 mmol of $Na^+B_5H_8^-$ in 40 mL of THF (prepared by deprotonation of B_5H_9 with NaH in THF) was added to the mixture through a sintered-glass filter on the vacuum line. The resulting mixture was stirred for 2 h at −63 °C, during which time it turned a dark green (nearly black) color. After solvent removal by rotavaporation, the residue was extracted with methylene chloride and the insoluble material removed by filtration. The workup of the filtrate was conducted as described for the preceding reaction, with preliminary separation on a silica column using hexane, 1:1 hexane/CH_2Cl_2, and pure CH_2Cl_2 to give one combined fraction and subsequent elution with 1:1 CH_2Cl_2/acetone to give a second fraction, which contained only red **1** (vide supra), yield 225 mg. The first fraction was placed on a preparative TLC plate and eluted with hexane followed by other solvents to give the following products. Cranberry $(Et_4C_4B_8H_8)Co(Et_4C_4B_8H_7OC_4H_8)$ (**3a**): yield ca. 10 mg; R_f (hexane) 0.83; high *m/e* 651 (parent, $^{13}C^{12}C_{27}{}^{11}B_{16}{}^{16}O^1H_{63}{}^{59}Co^+$, $C_{28}B_{16}OCo$ pattern). Golden $(Et_4C_4B_8H_7)_2Co_2$ (**2b**): yield 20 mg; R_f (1:1 CH_2Cl_2/hexane) 0.82; mp 93 ± 1 °C; high *m/e* 637 (parent, isomer of **2a**, vide supra); ^1H NMR (acetone-d_6) δ 0.72 (CH_3), 0.92 (complex multiplet, CH_3 + CH_2), 1.07 (CH_3). Orange $(Et_4C_4B_4H_6)CoH(Et_4C_4B_8H_8)$ (**5**): yield 83 mg; R_f (1:1 toluene/hexane) 0.54; high *m/e* 535 (parent, $^{13}C^{12}C_{23}{}^{11}B_{12}{}^1H_{55}{}^{59}Co^+$, $C_{24}B_{12}Co$ pattern); ^1H NMR ($CDCl_3$) δ 1.18 (CH_3), 2.40 (CH_2), 2.70 (CH_2). Orange $(Et_4C_4B_8H_7)_2CoH$ (**4a**): yield ca. 10 mg; R_f (3:2 toluene/hexane) 0.53; high *m/e* 579 (parent, $^{13}C^{12}C_{23}{}^{11}B_{16}{}^1H_{55}{}^{59}Co^+$, $C_{24}B_{16}Co$ pattern).

Isomerization of $(Et_4C_4B_8H_7)_2Co_2$ (2b) to 2c. A 30-mg sample of golden **2b** was placed in 1:1 hexane/toluene solution and stored under dry N_2 for 14 days at room temperature, during which the yellow solution turned brown. Removal of solvent and TLC with 1:1 hexane/CH_2Cl_2 gave 15 mg (50% yield) of a single product, purple-red **2c**: R_f 0.87; high *m/e* 637 (parent, isomeric with **2b**, vide supra).

Reaction of $(Et_4C_4B_8H_8)_2Co_2$ (1) with I_2. A 277-mg (0.43-mmol) sample of **1** was placed in a 100-mL flask, and 25 mL of acetone and 109 mg (0.43 mmol) of I_2 were added. The reactor was flushed with N_2, frozen in liquid nitrogen, and evacuated on the vacuum line. The reactor was warmed to room temperature and stirred overnight under an atmosphere of N_2. After removal of solvent by rotavaporation, the residue was placed on a silica gel column and eluted with hexane to give a dark brown solution. The solvent was stripped off, and the residue was placed on a TLC plate and eluted to give the following products. Purple-red $(Et_4C_4B_8H_7)_2(COMe_2)_2CoH$ (**3c**): yield 65 mg; R_f (hexane) 0.84; mp 162 + 1 °C; high *m/e* 695 (parent, $^{13}C^{12}C_{29}{}^{11}B_{16}{}^{16}O_2{}^1H_{67}{}^{59}Co^+$, $C_{30}B_{16}CoO_2$ pattern); ^1H NMR ($CDCl_3$) overlapping CH_3 and CH_2 multiplets between δ 0.8 and 1.4, sharp singlets (Me_2CO) at δ 1.552 and 2.172, unidentified sharp doublets at δ 1.765 (J = 6.8 Hz) and 2.037 (J = 6.5 Hz). Cherry $(Et_4C_4B_8H_7)_2(OH)Co$ (**3e**): yield 23 mg; R_f (hexane) 0.54; high *m/e* 595 (parent, $^{13}C^{12}C_{23}{}^{11}B_{16}{}^{16}O^1H_{55}{}^{59}Co^+$, $C_{24}B_{16}CoO$ pattern). Golden **2b** (vide supra): R_f (1:1 hexane/CH_2Cl_2) 0.82; yield 52 mg. Dark green $(Et_4C_4B_8H_7)_2(OH)Co$ (**3d**): yield 20 mg; R_f (1:1 hexane/CH_2Cl_2) 0.32; high *m/e* 595 (parent, isomer of **3e**, vide supra). Purple-red $(Et_4C_4B_8H_6OH)_2HCo$ (**3f**): yield 28 mg; R_f (1:1 acetone/CH_2Cl_2) 0.89; high *m/e* 611 (parent, $^{13}C^{12}C_{23}{}^{11}B_{16}{}^{16}O^1H_{55}{}^{59}Co^+$, $C_{24}B_{16}CoO_2$ pattern).

(20) Maynard, R. B.; Grimes, R. N. *Inorg. Synth.* **1983**, *22*, 215.
(21) Maxwell, W. M.; Bryan, R. F.; Grimes, R. N. *J. Am. Chem. Soc.* **1977**, *99*, 4008.

Table VI. Selected Bond Angles (deg) for 3c

B(2)-Co-B(2')	98.1 (2)	O(1)-B(3)-B(1)	130.7 (4)
B(2)-Co-B(3')	83.9 (2)	O(1)-B(3)-B(2)	124.8 (4)
B(3)-Co-B(2')	67.6 (3)	O(1)-B(3)-B(6)	127.6 (4)
C(1A)-O(1)-B(3)	132.1 (4)	O(1)-B(3)-B(9)	122.7 (4)
C(1A)-O(1)-B(2')	119.2 (4)	C(8)-B(4)-C(10)	101.5 (4)
B(3)-O(1)-B(2')	100.0 (3)	C(11)-B(12)-C(13)	100.5 (4)
C(2A)-O(2)-B(12')	124.1 (4)	Co-B(2')-O(1)	95.0 (3)
O(1)-C(1A)-C(1A1)	100.9 (5)	O(1)-B(2')-B(1')	126.8 (5)
O(1)-C(1A)-C(1A2)	110.5 (4)	O(1)-B(2')-B(3')	123.3 (4)
C(1A1)-C(1A)-C(1A2)	114.7 (5)	O(1)-B(2')-B(4')	122.4 (4)
O(2)-C(2A)-C(2A1)	104.9 (5)	O(1)-B(2')-C(8')	116.8 (5)
O(2)-C(2A)-C(2A2)	106.8 (4)	C(8')-B(4')-C(10')	95.8 (4)
C(2A1)-C(2A)-C(2A2)	112.2 (5)	B(12')-B(9')-C(11')	84.3 (3)
Co-C(8)-C(M8)	120.5 (3)	B(9')-B(12')-C(13')	130.8 (5)
C(M8)-C(8)-C(11)	120.7 (4)	Co-C(8')-C(M8')	126.9 (4)
C(M8)-C(8)-B(2)	122.8 (4)	B(2')-C(8')-C(M8')	129.2 (4)
C(M8)-C(8)-B(4)	107.8 (3)	B(4')-C(8')-C(M8')	102.9 (3)
C(11)-C(8)-B(4)	110.7 (4)	B(4')-C(8')-C(11')	117.5 (4)
C(8)-C(M8)-C(E8)	116.4 (4)	C(M8')-C(8')-C(11')	117.0 (4)
C(M10)-C(10)-C(13)	122.4 (5)	C(8')-C(M8')-C(E8')	119.7 (4)
C(M10)-C(10)-B(4)	116.7 (5)	B(4')-C(10')-C(M10')	114.6 (4)
C(M10)-C(10)-B(7)	125.8 (4)	B(4')-C(10')-C(13')	124.2 (4)
C(13)-C(10)-B(4)	120.5 (5)	B(7')-C(10')-C(M10')	136.7 (6)
C(10)-C(M10)-C(E10)	113.1 (5)	C(M10')-C(10')-C(13')	121.1 (4)
Co-C(11)-C(M11)	120.7 (4)	C(10')-C(M10')-C(E10')	102.3 (7)
C(8)-C(11)-B(12)	113.9 (4)	Co-C(11')-C(M11')	129.2 (4)
C(M11)-C(11)-B(9)	124.0 (4)	B(9')-C(11')-C(8')	114.7 (4)
C(M11)-C(11)-B(12)	107.7 (4)	B(9')-C(11')-C(M11')	125.6 (4)
C(11)-C(M11)-C(E11)	114.3 (6)	C(8')-C(11')-C(M11')	119.2 (4)
C(10)-C(13)-C(M13)	123.2 (5)	C(11')-C(M11')-C(E11')	117.0 (4)
C(10)-C(13)-B(12)	121.8 (5)	B(7')-C(13')-C(M13')	116.2 (5)
C(M13)-C(13)-B(7)	123.9 (5)	B(12')-C(13')-C(10')	120.8 (4)
C(M13)-C(13)-B(12)	114.1 (5)	B(12')-C(13')-C(M13')	114.6 (5)
C(13)-C(M13)-C(E13)	115.4 (5)	C(10')-C(13')-C(M13')	119.6 (5)
Co-B(3)-O(1)	96.9 (3)	C(13')-C(M13')-C(E13')	86.8 (7)

In a control experiment, a solution of **1** in acetone was stirred overnight under N_2 at room temperature, with no evidence of reaction. On removal of solvent, only compound **1** was recovered.

X-ray Structure Determination on $(Et_4C_4B_8H_8)_2(COMe_2)_2CoH$ (3c). Single crystals of **3c** were grown by slow evaporation from CH_2Cl_2 solution, and a selected crystal was mounted on a glass capillary and examined by precession photography, which showed it to be acceptable for data collection (parameters and crystal data are listed in Table III). The cell dimensions and space group were determined by standard methods on an Enraf-Nonius four-circle CAD-4 diffractometer equipped with a graphite monochromator, and the θ–2θ scan technique was employed as described elsewhere[22] to record the intensities of all nonequivalent reflections for which $1.5° < 2\theta < 52°$. Scan widths were calculated as $A + B \tan \theta$, where A is estimated from the mosaicity of the crystal and B allows for the increase in peak width due to $K\alpha_1$–$K\alpha_2$ splitting. The values of A and B were 0.60 and 0.35, respectively.

The intensities of three standard reflections showed no greater fluctuations during the data collection than those expected from Poisson statistics. The raw intensity data were corrected for Lorentz–polarization and absorption. Of the 6251 independent intensities, there were 3054 with $F_o^2 > 3\sigma(F_o^2)$, where $\sigma(F_o^2)$ was estimated from counting statistics.[23] These data were used in the final refinement of the structural parameters.

Solution and Refinement of the Structure. A three-dimensional Patterson synthesis was used to determine the heavy-atom position, which phased the data sufficiently well to permit location of the remaining non-hydrogen atoms from Fourier syntheses. Two carborane cages, coordinated to cobalt, were found to be linked by an atom identified from its electron density as the oxygen of an acetone molecule. Some positional disorder was observed in the cage ethyl groups. Least-squares refinement was carried out as previously described.[22] Anisotropic temperature factors were introduced for the non-hydrogen atoms. Further Fourier difference functions permitted location of some non-methyl hydrogen atoms, which were included in the refinement for four cycles of least-squares refinement and then held fixed.

The model converged with $R = 0.073$ and $R_w = 0.084$. A final Fourier difference map was featureless. A listing of the observed and calculated structure factors is available together with calculated thermal parameters.[24]

Acknowledgment. The assistance of Dr. T. L. Venable in obtaining ^{11}B NMR spectra and of Dr. Jeffrey Shabanowitz in recording some of the mass spectra is gratefully acknowledged. This work was supported by the National Science Foundation, Grant No. 81-19936.

Supplementary Material Available: Listings of observed and calculated structure factors, anisotropic thermal parameters, and calculated mean planes (17 pages). Ordering information is given on any current masthead page.

(22) Freyberg, D. P.; Mockler, G. M.; Sinn, E. *J. Chem. Soc., Dalton Trans.* **1976**, 447.
(23) Corfield, P. W. R.; Doedens, R. J.; Ibers, J. A. *Inorg. Chem.* **1967**, *6*, 197.
(24) Supplementary material.